Absorption of He–Ne Laser Radiation in an Exploded Lithium-Wire Plasma*,†

EROL OKTAY‡ AND DAVID R. BACH

Nuclear Engineering Department, The University of Michigan, Ann Arbor, Michigan 48105

(Received 13 August 1969; in final form 20 November 1969)

Calculations of the absorption coefficients for inverse bremsstrahlung in the field of ions and neutral atoms in ground and excited states and for photoionization are presented for the absorption of He–Ne laser radiation in dense Li plasmas. These are compared with those measured in an exploded Li-wire plasma and the two values differ at most by a factor of five. The electron density and temperature in the plasma are estimated from the time-resolved spectroscopic measurements using the Stark broadening of the Li 6103 line and the intensity ratios of various neutral and ionized Li lines. The plasma diameter and the total neutral atom densities are estimated from the framing and streak pictures of the plasma.

I. INTRODUCTION

Significant absorption of ruby laser radiation has been observed in laser-induced gas-breakdown experiments.[1–6] In very few cases, however, have the measured values of optical absorption been directly compared with the calculated values. Litvak and Edwards[7] reported a measured absorption coefficient 100 times greater than that calculated; Lampis and Brown[8] reported a discrepancy of a factor of 80 in the opposite direction in their experiment. These discrepancies motivated us to study specifically the optical absorption phenomena in dense plasmas. A theoretical study in this area was conducted in the Nuclear Engineering Department of The University of Michigan[9,10] and an experiment was therefore designed to study the absorption of He–Ne laser radiation in an exploded lithium-wire plasma.

In Sec. II of this paper, the optical processes are briefly reviewed, and numerical calculations of the absorption coefficients for the absorption of He–Ne laser radiation in Li plasmas are presented.

In Sec. III the absorption measurement is discussed and includes a description of the methods used for estimating plasma diameter, electron and neutral atom densities, and electron temperatures.

In Sec. IV the experimental values of the absorption coefficients are compared with those calculated.

II. THEORY OF PHOTON ABSORPTION IN PARTIALLY IONIZED PLASMAS

In passing through the plasma, the incident radiation may be absorbed, reflected, scattered, or refracted. In this section we give a brief discussion of the absorption process.

Photons may be absorbed in a system which contains free electrons, free ions, and neutral atoms. The photon absorption is accompanied by an electronic transition in the system which may be

(i) bound–bound,
(ii) free–free, or
(iii) bound–free.

Since we are interested in the interaction of He–Ne laser radiation with a Li plasma, we need to consider only bound–free and free–free transitions. There are no two energy levels in lithium whose energies differ by 1.96 eV, which is the photon energy of 6328-Å He–Ne laser radiation, and therefore, bound–bound transitions (line absorptions) do not occur.

Absorption of photons due to the presence of negative Li ions, Li^-, via free–free (inverse bremsstrahlung of

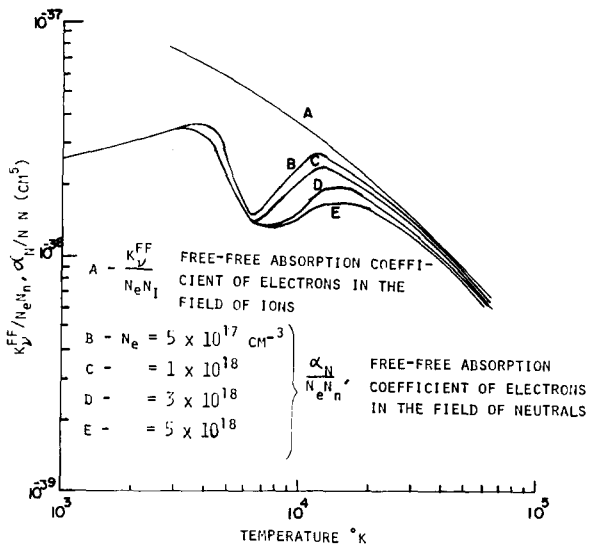

FIG. 1. Absorption coefficients of inverse bremsstrahlung in the field of ions and neutral atoms as functions of temperature and electron density.

electrons in the field of negative ions) or bound–free (photo-detachment) transitions was expected to be negligible in this experiment. Quoted values[11,12] for the electron affinity of Li vary from 0.3 to 0.8 eV, and since the temperature in the exploding Li-wire plasma produced in this experiment is larger than 0.8 eV, the probability of the existence of Li^- is small. Furthermore, large numbers of negative ions can only be formed if there are impurity atoms in the plasma which have

lower ionization potentials than those of the atoms converting to the negative ion.[13] Since such impurities do not exist in exploding Li plasmas, the density of the negative ions was expected to be negligible.

In this paper, therefore, we will consider only the following absorption mechanisms:

(i) inverse bremsstrahlung in the presence of positive ions free–free),

(ii) inverse bremsstrahlung in the presence of neutral atoms in ground and excited states (free–free), and

(iii) photoionization (bound–free).

A. Inverse Bremsstrahlung of Electrons in the Field of Positive Ions

The derivation of the absorption coefficient of inverse bremsstrahlung in the presence of positive ions, K_ν^{ff}, is well known. The expression for K_ν^{ff} is given as follows[14]:

$$K_\nu^{ff}=\frac{16\pi}{3^{3/2}}\frac{c^2}{h}(\alpha a_o)^3 E_H^{3/2}\frac{N_I N_e}{\theta^{1/2}}\frac{g_{ff}}{\nu^3}(1-e^{-h\nu/\theta}), \quad (1)$$

where

c	3×10^{10} cm/sec, the speed of light
h	6.63×10^{-34} J-sec, Planck constant
α	1/137, fine structure constant
a_0	0.53 Å, first Bohr radius
E_H	13.6 eV, Rydberg constant
θ	kT (eV)
k	1.38×10^{-23} J/°K, Boltzman constant
T	electron temperature (°K)
Z	ion charge (for singly ionized Li, $Z=1$)
N_I, N_e	ion and electron densities
g_{ff}	free–free Gaunt factor
$(1-e^{-h\nu/\theta})$	correction term for induced emission.

The values of g_{ff}, which are functions of h_ν and T, have been tabulated by Karzas and Latter.[15] Using these, the values of g_{ff} were determined for $h\nu=1.96$ eV, and for temperatures between 5×10^3 and 5×10^4°K. The absorption coefficient, K_ν^{ff}/N_eN_I, was then calculated for $h\nu=1.96$ as a function of temperature, T, Fig. 1.

B. Inverse Bremsstrahlung of Electrons in the Field of Neutral Atoms

While much attention has been given to free–free transitions in the field of ions, very little work has been done on electronic transitions in the field of neutral atoms. The main contribution to these studies has come from astrophysicists who have concerned themselves with the absorption of continuum radiation of the sun in the stellar atmosphere.[16–18] These studies, however, have been limited to hydrogen atoms and to temperatures below 10^4°K. At these temperatures, the hydrogen atom is mainly in the ground state. Therefore, the calculations included inverse bremsstrahlung in the presence of nonexcited neutrals. In the past few years, further studies in this area were carried out by Akcasu and Wald,[19] Firsov and Chibisov,[20] Kivel,[21] and by Mjolness and Ruppel,[22] who also considered the contribution of nonexcited neutrals. In laboratory plasmas with temperatures as high as 2×10^5°K, most of the neutral atoms are in highly excited states. It was expected that the presence of these excited neutral atoms would significantly alter the photon absorption.

Recently Tsai, Akcasu, and Osborn[9] calculated the contribution of neutral atoms at high temperatures and in excited states to the photon absorption in hydrogen plasmas through inverse bremsstrahlung of electrons. They obtained the following expression for the absorption coefficient for this process, α_N:

$$\alpha_N(h\nu, T)=C_0(e^{h\nu/\theta}-1)h\nu N_e\sum_{n=1}^{n^*}g_{nn}(h\nu, T)N(n), \quad (2)$$

where

$$C_0=\frac{4}{3\sqrt{2}}\frac{\hbar^2c^2\alpha^3}{(\pi m\theta)^{3/2}}\frac{1}{\nu^3},$$

m is the electron mass, $N(n)$ is the number density of neutral atoms in nth excited state, and g_{nn} is related to the collision cross sections of electrons with neutral atoms in the nth excited state. A correction due to induced emission is included in this expression. The results of numerical calculations for the absorption of ruby laser radiation can be found in Ref. 10. In calculating the absorption in the field of Li atoms, it was assumed that the properties (electron–atom collision cross section) of the Li atom in the ground state, $2^2S_{1/2}$, were reasonably well approximated by a hydrogenic calculation with $n=2$.

In Eq. (2), the sum was calculated from $n=2$ to n^*, where n^* is the highest state a neutral atom can be in without being ionized under the given conditions of the plasma. Atoms in excited states $n>n^*$ were considered free ions and electrons.

1. Evaluation of g_{nn}

Tsai *et al.*[9,10] calculated g_{nn} for $n=1$, 2, and 3 as functions of temperature and photon energy. The values of g_{nn} were determined from their results for $h\nu=1.96$, $n=1$, 2, and 3 and are plotted as functions of temperature in Fig. 2. At the temperatures attained in the exploding Li-wire plasma produced in this experiment, a large percentage of neutral atoms may be in excited states above $n=3$; therefore, the values of g_{nn} for $n>3$ were required.

First, the values of g_{nn} for $n=\infty$, $(g_{\infty\infty})$ were calculated as functions of temperature.[9,10] The results are also plotted in Fig. 2. These were obtained by equating K_ν^{ff}/N_I in Eq. (1) to $\alpha_{nn}/N(n)$ in Eq. (2):

$$\alpha_N=\sum_{n=1}^{n^*}\alpha_{nn}.$$

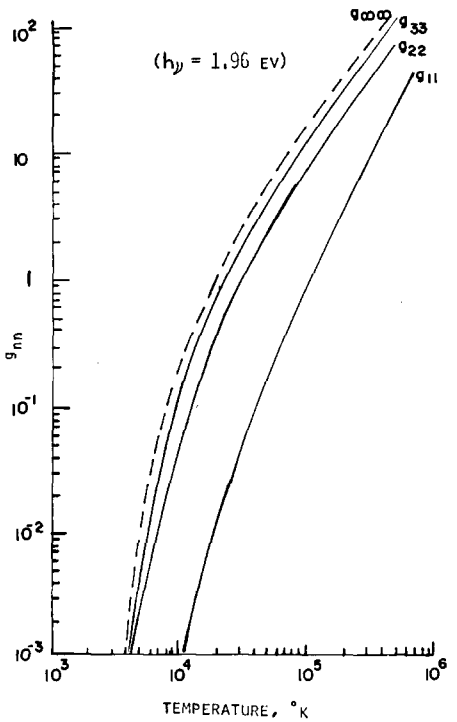

FIG. 2. g_{nn} versus temperature for $h\nu = 1.96$ eV.

To evaluate g_{nn} for $n > 3$, values of g_{nn} for $n = 1, 2, 3$ and ∞ were plotted as a function of $1/n^2$ at a given temperature. The values of g_{nn} for any n at that temperature were then determined from this curve. These curves of g_{nn} for temperatures 10^4 to 5×10^4 are shown in Fig. 3.

2. *Evaluation of n**

The value of n^* approaches ∞ for an isolated atom. In a plasma, neutral atoms are surrounded by free electrons and ions which lower the ionization potentials[23,24] and perturb the energy levels. If we assume that these neutral atoms in the plasma can still be approximated by hydrogen-like atoms, which have ionization potentials lower than E_∞, then the value of n^* must be a finite number.

There is no precise method which can be used to determine the value of n^*.[23,25,26] However, two possible limits which have been used to determine the radius (therefore n^*) of the excited neutral atom are the Debye length and the interatomic distance.[26,27] The first yields a value of n^* similar to that obtained by calculating the lowering of the ionization potential,[28] and we used this method. In Fig. 4, the Debye radius is plotted as a function of a plasma parameter, θ/N_e, where $\rho^D = (\theta/8\pi N_e e^2)^{1/2}$, and on this graph the approximate radii of excited atoms in the nth states are shown. The radii are given approximately by $r_n = n^2 a_0$, where a_0 is the first Bohr radius. For given values of N_e and θ, the value of n^* is thus determined from this graph.

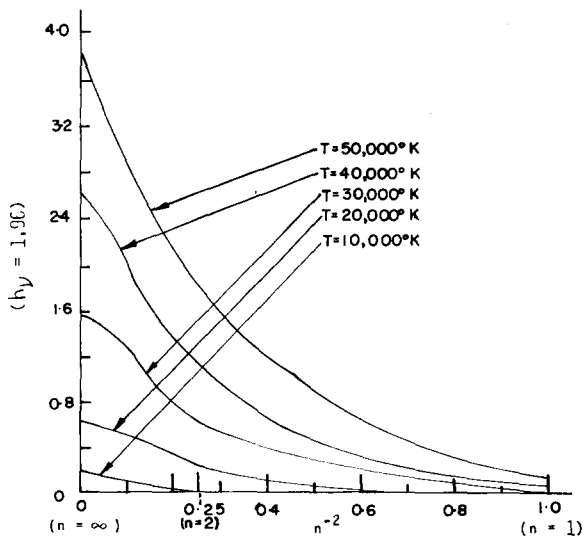

FIG. 3. $g_{nn}(h\nu = 1.96$ eV) versus n^{-2} for various temperatures.

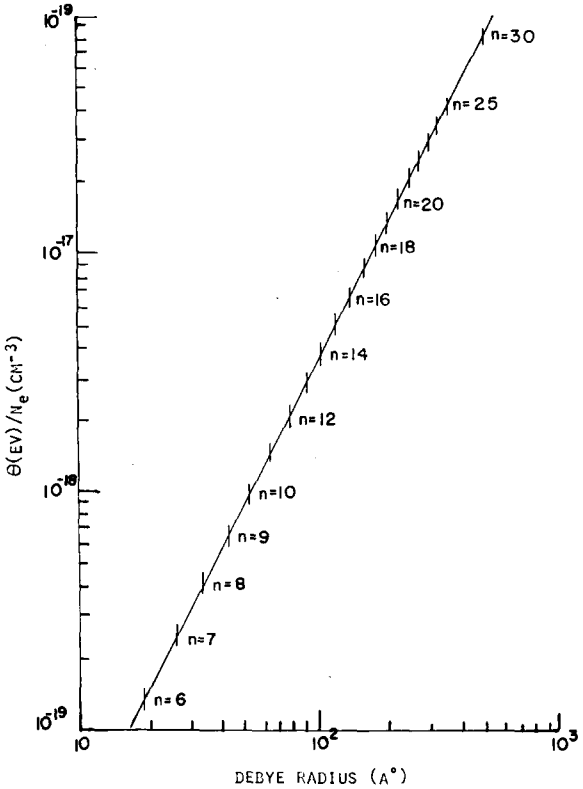

FIG. 4. θ/N_e versus Debye and excited atom radii.

3. *Evaluation of N(n)*

The Boltzmann factor was used to calculate the density of neutral atoms in the nth excited state, $N(n)$.

This factor relates the densities of atoms in the nth and mth states[24]:

$$\frac{N(n)}{N(m)}=\frac{g_n}{g_m}\frac{\exp(-E_{ne}/\theta)}{\exp(-E_{me}/\theta)}, \tag{3}$$

where g_n and g_m are the statistical weights of levels n and m; and, E_{ne} and E_{me} are the excitation energies of these levels. The total neutral atom density N_n, is given by

$$N_n=\sum_{n=1}^{n^*}N(n).$$

The relative density of neutral atoms in the nth excited state with respect to total neutral atom density is given by

$$N(n)/N_n=g_n\exp(-E_{ne}/\theta)/U, \tag{4}$$

where U is the partition function, defined as

$$U=\sum_{n=1}^{n^*}g_n\exp\left(\frac{-E_{ne}}{\theta}\right). \tag{5}$$

The values of g_n and E_{ne} are tabulated in Ref. 29 for $n<13$. For $n>13$, $g_n=2n^2$ and $E_{ne}=5.31$ were used.

Thus, for a given electron temperature and density, the values of n^*, g_{nn}, and $N(n)/N_n$ were determined, and then α_N/N_eN_n was calculated using Eq. (2). The results are shown graphically in Fig. 1 and deped on electron density since the value of n^* is a function of the electron density.

The variation of the value of α_N/N_eN_n with different values of n^* is no larger than a few percent when n^* is greater than about 8. This is because the expression for α_N/N_eN_n includes like sums in both numerator and denominator. Equation (2) can be written as follows:

$$\alpha_N/N_eN_n=f(\theta)\sum_{n=1}^{n^*}g_{nn}N(n)/\sum_{n=1}^{n^*}N(n). \tag{6}$$

For $n>8$ the value of g_{nn} approaches a constant value, $g_{\infty\infty}$; therefore, α_N/N_eN_n is insensitive to the value of n^*.

In Fig. 1, the absorption coefficient for inverse bremsstrahlung in the presence of ions, K_ν^{ff}/N_eN_i, is compared to that absorption coefficient for inverse bremsstrahlung in the presence of neutrals, α_N/N_eN_n. At high temperatures, the two coefficients become almost equal because the fraction of neutrals in higher excited states becomes large and these highly excited neutrals act like ions. Similarly, α_N/N_eN_n increases as electron density decreases because n^* increases as the N_e decreases.

In Ref. 9, values of g_{nn} are given only for $T\geq5000$°K. Therefore, calculations described above were made for temperatures greater than 5000°K. In order to calculate α_N/N_eN_n for $T<5000$°K, the equation derived by Akcasu and Wald[19] was used. This equation is

$$\frac{\alpha_{\text{eff}}}{N_eN_n}=\frac{c^2\pi^2}{(2\pi\nu)^3}\frac{4\alpha}{3\pi}\left(\frac{2}{\pi m\theta}\right)^{1/2}\frac{\sigma(0)}{m}\left(\frac{h\nu}{c}\right)^2\times K_2\left(\frac{h\nu}{2\theta}\right)e^{-h\nu/2\theta}(e^{h\nu/\theta}-1), \tag{7}$$

where $\sigma(0)$ is the low-temperature limit of electron–atom collision cross section, and $K_2(h\nu/2\theta)$ is the second-order Bessel function. This equation was derived for the absorption of photons in low-temperature plasmas by inverse bremsstrahlung of electrons in the presence of ground-state neutrals.

There is about 25% difference between the values of $\alpha_{\text{eff}}/N_eN_n$ and α_N/N_eN_n at $T=5000$°K. However, this difference was not significant in view of the errors in this experiment. An average curve was drawn to obtain a continuous curve for the absorption coefficient from $T=10^3$ to 5×10^4°K.

C. Photoionization

The cross section for the photoionization of a hydrogen-like atom in an excited state n is given by[24]

$$\sigma_{\nu n}^{bf}=(64\alpha/3^{3/2})\pi a_0^2(E_H/h\nu)^3n^{-5}g_{bf}, \tag{8}$$

where g_{bf} is the bound–free Gaunt factor. The values of g_{bf} have been tabulated by Karzas and Latter[15] and they are approximately unity for the present experiment.

The absorption coefficient, K_ν^A, is obtained by multiplying $\sigma_{\nu n}^{bf}$ by $N(n)$, and summing over all n's:

$$K_\nu^A=\sum_{n=h}^{n^*}\sigma_{\nu n}^{bf}N(n). \tag{9}$$

In order to evaluate the expression for the net absorption coefficient, the contribution of induced emission had to be included. In the derivation of absorption coefficients for inverse bremsstrahlung, the expression $(1-e^{-h\nu/\theta})$ was used for this correction. Use of this expression for the photoionization process implies that electron, ion, and neutral atom densities are related by the Saha equation. When the Saha equation cannot be reliably applied, as in the present experiment, the induced-emission term must be modified since the photoionization coefficient is proportional to the densities of excited neutral atoms, $N(n)$, while the induced emission (radiative recombination) is dependent on electron and ion densities. It can be shown, starting from quantum-mechanical transition probabilities for absorption and for induced emission, and assuming that electrons, ions and neutral atoms have Maxwellian velocity distributions, that the correction term for induced emission should be[10]

$$\left[1-\frac{N_eN_I}{N_n}\left(\frac{h^2}{2\pi m\theta}\right)^{3/2}\tfrac{1}{2}U\exp\left(\frac{E_\infty}{\theta}\right)\exp\left(\frac{-h\nu}{\theta}\right)\right], \tag{10}$$

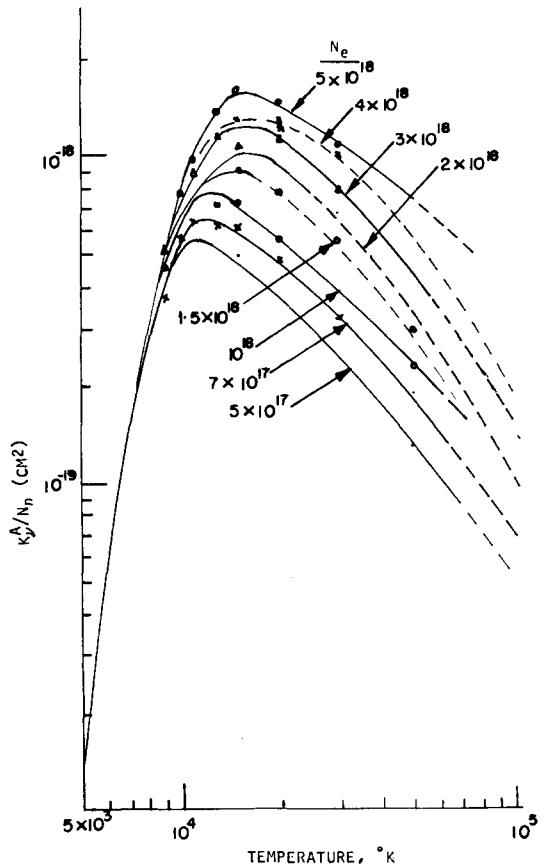

FIG. 5. Absorption coefficient of photionization as functions of temperature and electron density.

where E_∞ is the ionization potential of the atom. This expression reduces to $(1-e^{-h\nu/\theta})$ if the Saha equation is used. Thus, for the system in which the Saha equation is not applicable, the net absorption coefficient for photoionization is given by

$$\alpha^{PI}=\frac{64\alpha}{3^{3/2}}\pi a_0^2\left(\frac{E_H}{h\nu}\right)^3\sum_{n=k}^{n^*}n^{-5}N(n)$$

$$\times\left[1-\frac{N_eN_I}{N_n}\left(\frac{h^2}{2\pi m\theta}\right)^{3/2}\tfrac{1}{2}U\exp\left(\frac{E_\infty}{\theta}\right)\exp\left(\frac{-h_\nu}{\theta}\right)\right], \quad (11)$$

which can be written as

$$\alpha^{PI}=K_\nu^A-K_\nu^{IE}. \quad (12)$$

We approximated the Li atom by an H atom and used Eq. (12) to calculate the photoionization absorption coefficients. Exact calculations of photoionization cross-sections have been carried out for the first few levels of Li by Gezalov and Ivanova[30] and by Ya'akobi,[31] and their results do not differ from those obtained by the hydrogen-like approximation by more than 20%–30%.

The level $n=k$ represents the lowest level from which photoionization can take place. Since the incident photon energy is 1.96 eV, only Li atoms in excited levels $3p$ and above can be photoionized and the summation for α^{PI} begins at $k=3p$.

Numerical calculations of α^{PI} were made in two steps. First the values of K_ν^A, which is the absolute absorption coefficient, were calculated. K_ν^A is a function of the total neutral atom density N_n. The results of these calculations are plotted as K_ν^A/N_n versus T in Fig. 5. Subsequently, the correction due to induced emission, which is a function of the electron and ion densities, was calculated. The results K_ν^{IE}/N_eN_I are plotted as a function of T, Fig. 6. In order to determine a value for the net absorption coefficient due to photoionization, the value of K_ν^{IE} is subtracted from that of K_ν^A. The correction due to induced emission is strongly dependent on the particle densities and temperature in the plasma. It can be large when $T<5000$°K.

K_ν^A/N_n first increases with temperature, reaches a peak and then decreases rapidly with temperature. At low temperatures most of the atoms are below the $3p$ level. As the temperature increases, the percentage of atoms in states $3p$ to 8 increases rapidly; therefore, the absorption coefficient increases. As the temperature increases further, the atoms are excited to still higher levels, $(n\gtrsim 8)$. However, the contribution of these atoms to photoionization is small because the coefficient varies as $1/n^5$. Therefore, K_ν^A/N_n finally decreases with temperature.

The value of n^* affects the K_ν^A/N_n significantly. The expression in Eq. (11) for K_ν^A can be written as

$$K_\nu^A=C\times\sum_{n=k}^{n^*}n^{-5}N(n) \qquad C \text{ is a constant.} \quad (13)$$

It can be shown that

$$K_\nu^A/N_n=C\times\sum_{n=k}^{n^*}n^{-3}\exp\left(\frac{-E_{ne}}{\theta}\right)\Big/U, \quad (14)$$

where U is the partition function [Eq. (5)]. The value of g_n in this equation varies as $2n^2$. The numerator of

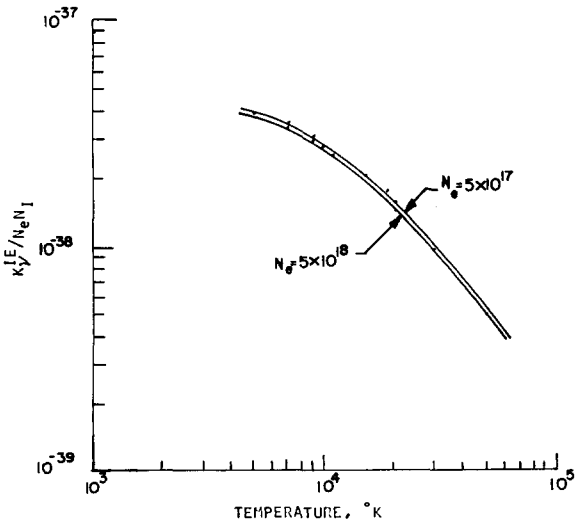

FIG. 6. Induced-emission correction to photoionization absorption coefficient as functions of temperature and electron density.

Eq. (14) becomes constant as n approaches 8. (The value of U, on the other hand, increases rapidly.) Therefore, when n is larger than about 8, the $K_\nu{}^A/N_n$ varies approximately as $1/U$, which depends on the value of n^*. The curves in Fig. 5 are therefore strongly dependent on N_e because of the n^* dependence.

In summary, the values of absorption coefficients for inverse bremsstrahlung in the presence of ions ($K_\nu{}^{II}/N_eN_I$), and neutrals (α_N/N_eN_n) and for photoionization ($\alpha^{PI}=K_\nu{}^A-K_\nu{}^{IE}$) were evaluated and plotted as functions of temperature and electron densities for the absorption of the He–Ne laser radiation ($\lambda=6328$ Å, $h\nu=1.96$ eV) in Li plasmas. If the plasma parameters (N_e, N_n, T) are known, the absorption coefficient for a particular plasma can be easily predicted using these results.

Since the absorption coefficients are given in terms of per particle densities, they are applicable to any Li plasma in which the Saha equation may or may not prevail. If the Saha equation is not applicable, then the total neutral atom density has to be determined independently of the electron density.

III. ABSORPTION MEASUREMENT

An exploding Li-wire plasma was used to study the absorption of the He–Ne laser radiation. Electron densities of 5×10^{18} cm^{-3} and temperatures of about 5×10^4°K can be produced in these partially ionized plasmas and these conditions are suitable for the absorption of optical radiation.

Whereas in the typical absorption experiment using a laser-produced plasma, the same laser pulse is used to produce the plasma and to study its absorption in that plasma, the sources of energy producing the plasma and the laser radiation were separated in this experiment.

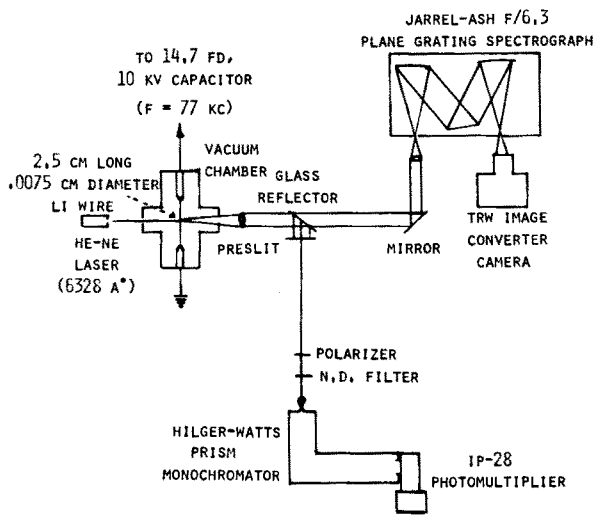

FIG. 7. A schematic of the experimental arrangement to measure the absorption of He–Ne laser radiation in an exploded Li-wire plasma.

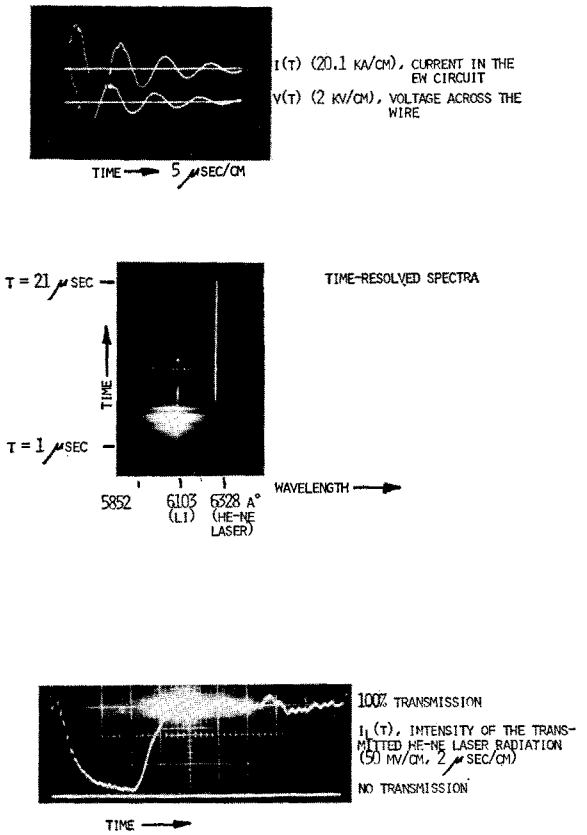

FIG. 8. Typical data of the absorption measurement.

The power of the laser beam (2 mW) was much less than that used in the production of the plasma (the order of megawatts); therefore, perturbation of the plasma by the laser radiation was negligible.

The plasma geometry was cylindrical for about 6 μsec which assisted in the interpretation of the experiment.

Since the He–Ne laser radiation was incident on the plasma continuously, the absorption measurements were made over the entire duration of the plasma (a few microseconds). The plasma varied significantly over this period and the absorption measurements could therefore be made in a plasma having varying parameters during one wire explosion.

In order to compare the experimental and theoretical absorption, it was necessary to measure the electron and neutral atom densities, the temperature, and the size of the plasma column. The electron temperature and density were estimated from the time-resolved spectroscopic measurements; the size of the plasma column and the neutral atom densities were estimated from streak and framing pictures of the plasma.

A. Description of the Experimental Arrangement

In Fig. 7 a schematic of the experimental arrangement is shown. Li wire was exploded in a vacuum chamber and the He–Ne laser radiation was passed

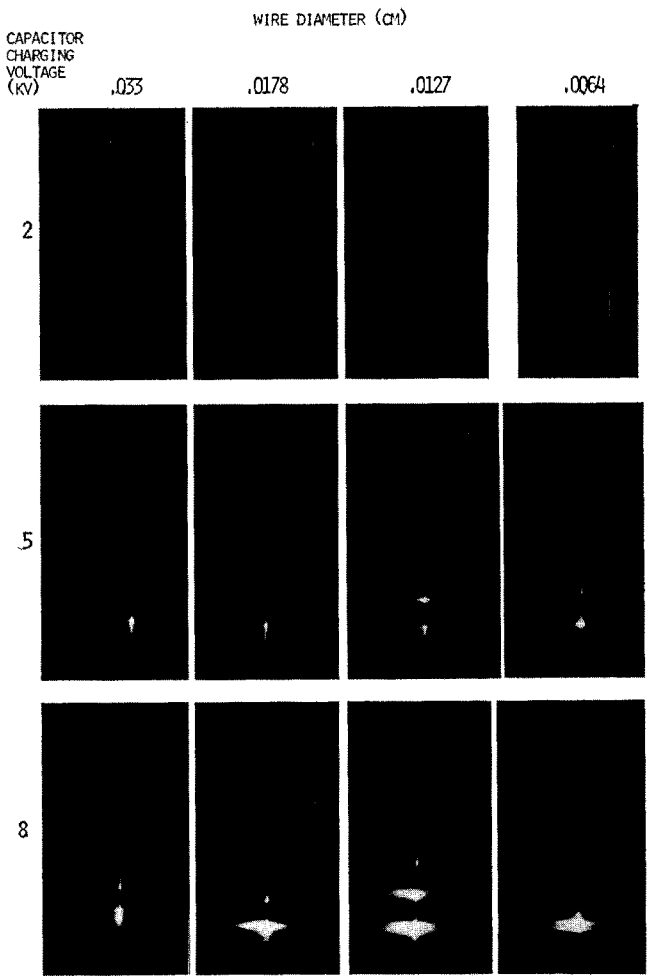

FIG. 9. Time-resolved spectra and the absorption of He–Ne laser radiation for various wire diameters and capacitor changing voltages. (Streak time: 1 to 50 μsec.)

through the plasma. A Jarrel Ash $f/6.3$ plane grating (30 000 lines/in.) spectrograph and a TRW Image Converter camera were used to obtain time-resolved spectra of the radiation emitted by the plasma. The Hilger–Watts prism monochromator and a I-P 28 photomultiplier were used to measure the intensity of the laser radiation transmitted through the plasma.

In the exploding wire circuit, a 13.8 μF/20 kV capacitor was used as the energy-storage capacitor. The ringing frequency of this circuit was 77 kHz. The voltage across the wire, $v(t)$, was measured with a Tektronix P-6015 high-voltage probe. The current in the circuit, $i(t)$, was measured with a T & M F-2500 current viewing resistor which had 0.00285-Ω resistance.

Lithium wire is commercially available only in 0.317-cm diameter. In these experiments, a wire diameter of only a few thousands of centimeters required. Therefore a die-electrode combination was developed which made it possible to reduce the diameter of the wire from 0.317 to 0.0023 cm.[32–34]

The explosions were made in vacuum (about 10 mTorr) because: (a) the reaction of Li with water vapor in air was minimized, (b) the spectra of the explosions in vacuum consisted of line radiation which was simple to analyze, and (c) the density of ambient gas was kept low in order to prevent any appreciable absorption of He–Ne laser radiation in the shock-front outside of the plasma column.

Oscilloscope recordings of the typical $v(t)$ and $i(t)$ traces for the explosion of a 0.0127-cm-diam, 2.5-cm-long Li wire in vacuum are shown in Fig. 8. (The capacitor was charged to 10 kV. The discharge was an oscillatory one, characteristic of L–R–C circuits.) The three states (first pulse—dwell—restrike) which occurs when the wire is exploded in atmospheric pressures do not occur in explosions conducted in vacuum.

B. Optical Arrangement

The radiation from the plasma and the transmitted laser radiation were collected with lens L_1 (Fig. 7). Some of this radiation was reflected into the monochromator by a glass slide. A pre-slit with a 1-mm-diam hole was placed between the glass slide and the mono-

chromator at the point where the laser came into focus to block most of the plasma radiation. The intensity of plasma radiation passing through the hole was further minimized by placing a polarizer in front of the monochromator. In addition, the exit slit of the monochromator was centered on the He–Ne 6328-Å radiation. Thus, the photomultiplier recorded only the intensity of the transmitted laser radiation I_L. A typical absorption trace is shown in Fig. 8.

The direct radiation was focused on the entrance slit of the spectrograph with the use of a front-surface mirror and two lenses. The image converter camera was focused on the exit slit of the spectrograph.

The dispersion on the photographic plate obtained with the image converter camera was about 16 Å/mm, and the wavelength range that could be photographed was about 400 Å. A typical time-resolved spectrum thus obtained is shown in Fig. 8. The incident laser radiation, which is absorbed during a period of the discharge, is also included in this spectrum.

In Figs. 9 and 10, time-resolved spectra and the absorption of He–Ne laser radiation are shown for plasmas produced by exploding wires with various wire diameters and capacitor charging voltages. These pictures indicate that the duration of absorption of the laser radiated was significantly affected by the values of these parameters. Absorption continued for the longest periods of time (40–50 μsec) when wire diameter was large (0.025–0.033 cm) and charging voltage was low (2–5 kV).

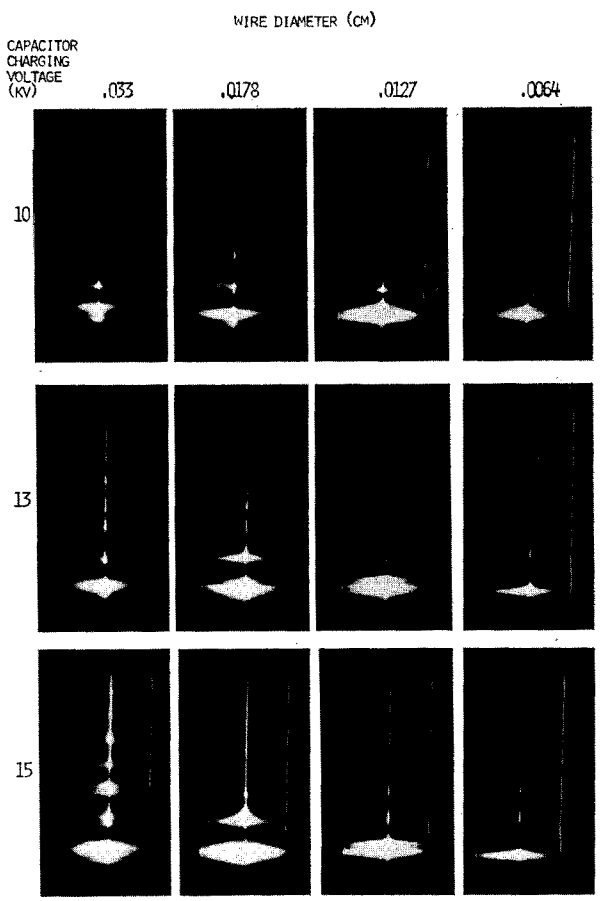

FIG. 10. Time-resolved spectra and the absorption of He–Ne laser radiation for various wire diameters and capacitor charging voltages. (Streak time 1 to 50 μsec.)

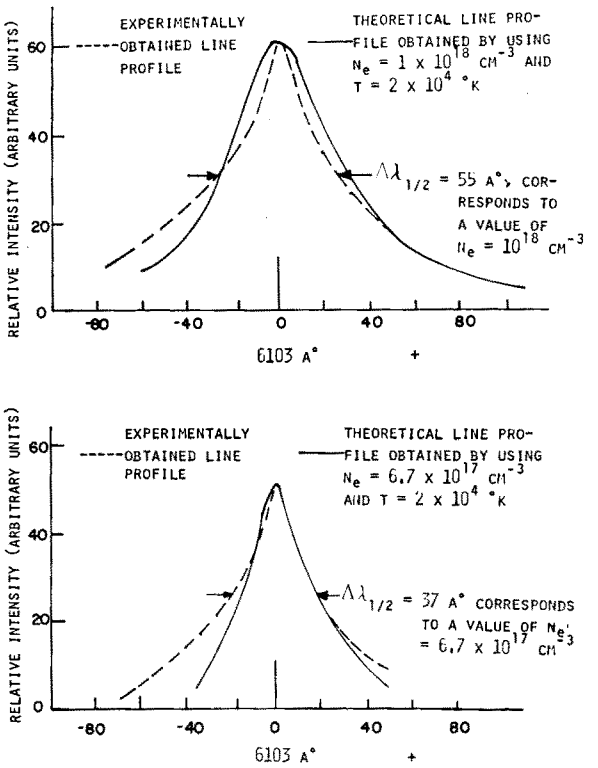

FIG. 11. Experimental and theoretical line profiles of the Li 6103 line for two different electron densities.

It was decided to analyze a case in which absorption lasted about 6 μsec since meaningful measurements of the plasma parameters could be made only during this period. After this time, the plasma column rapidly dispersed and the plasma diameter and neutral atom densities could not be measured accurately. Therefore, a 0.0075-cm-diam, 2.5-cm-long wire was used and the capacitor was charged to 10 kV. The following discussion is for measurements which were made under these experimental conditions.

C. Time-Resolved Spectroscopic Measurements

Electron density and temperature were estimated from the time-resolved spectroscopic measurements. Stark broadening of the Li 6103 line was measured as a function of time to determine the electron density; intensity ratios of various neutral and ionized Li lines were measured to estimate upper and lower limits of electron temperature.

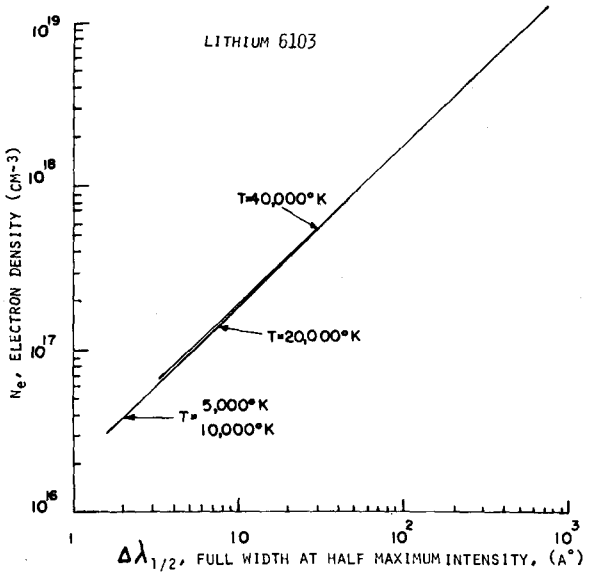

FIG. 12. Electron density versus the Stark broadening of the Li 6103 line.

Kodak Royal X-Pan film was used to record the spectra which was developed in Acufine developer to raise the speed of the film to ASA 3000. The film was calibrated for intensity by recording the intensity of He–Ne laser radiation at varying streak rates and intensities. The intensity of the laser was varied by using neutral density filters.

1. Estimate of Electron Density

The spectra were analyzed by use of a microdensitometer. In Fig. 11, typical experimental profiles of the Li 6103 line are shown at two different stages of the discharge. The value of full-width at half-intensity maximum, $\Delta\lambda_{1/2}$ of these line profiles were used to obtain values for the electron density. In Fig. 12, electron density versus $\Delta\lambda_{1/2}$ are plotted. Griem's[24] data on Stark broadening of Li 6103 were used to obtain this plot. The Stark broadening of this line is insensitive to temperature. Theoretical line shapes are also shown in Fig. 11 which were obtained by using the values of electron densities from the measurement of the width.

Comparison of the experimental line profiles with theoretical line shapes which take into account self-absorption[35] indicate that the error in the density determination due to the self-absorption is less than about 25%.

Figure 13 shows the temporal variation of electron density obtained by the above method. Electron density increased to about 4.2×10^{18} cm^{-3} in the first three microseconds, and then decreased with time. Measurements were made during the first 7 μsec of the discharge, since the absorption of the He–Ne laser radiation in the plasma took place during this time.

2. Estimate of Electron Temperature from Line Intensity Ratios

The ratios of various neutral line intensities were calculated as a function of T, using the expression[24]

$$\frac{I_T}{I_{T'}}=\left(\frac{\lambda'}{\lambda}\right)^3\frac{g_l f_{lu}}{g_l' f_{lu}'}\exp\left(\frac{E_u'-E_u}{\theta}\right). \tag{15}$$

These lines had the identical lower energy level, $2^2P_{3/2\,1/2}$. Some of the results are shown in Fig. 14. These calculations indicated that the values of the intensity ratios were insensitive to temperature when T was higher than about 10^4°K.

The intensity ratios of some of these lines observed in the time-resolved spectra indicated temperatures higher than 10^4°K.

The intensity ratios of ionized to neutral atom lines were also examined, using the equation[24]

$$\frac{I_T'}{I_T}=\frac{f_{lu}'}{f_{lu}}\frac{g_l'}{g_l}\frac{\lambda^3}{\lambda'^3}(4\pi^{3/2}a_0^3N_e)^{-1}\left(\frac{\theta}{E_H}\right)^{3/2}$$

$$\times\exp\left(-\frac{E_u'+E_\infty-E_u-\Delta E_\infty}{\theta}\right), \tag{16}$$

where the primed quantities refer to the ionized atom lines. Some of these calculations are shown in Fig. 15.

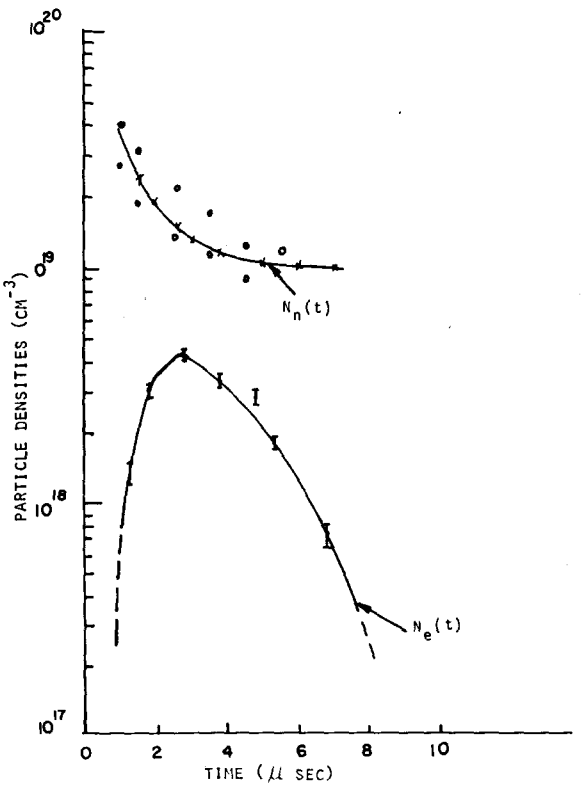

FIG. 13. Neutral atom and electron densities as functions of time for the explosion of a 0.0075-cm-diam, 2.5-cm-long Li wire in vacuum with V_0-10 kV.

This method is suitable for temperatures above about 4×10^4°K. Below these temperatures, the intensity ratios are very small and cannot be measured.

Examination of various line ratios revealed that the intensity of the ionized atom line was never greater than that of the neutral atom line, Li 4602. Therefore, the upper limit of the temperature in the plasma was about 5×10^4°K.

These two line-intensity-ratio methods yield a peak temperature range between 10^4 to 5×10^4°K. Since meaningful time-dependent estimates of temperature could not be obtained, three different temperature variations with time were assumed, Fig. 16. This was done in order to calculate values of absorption as a function of time and compare these with the experimental values.

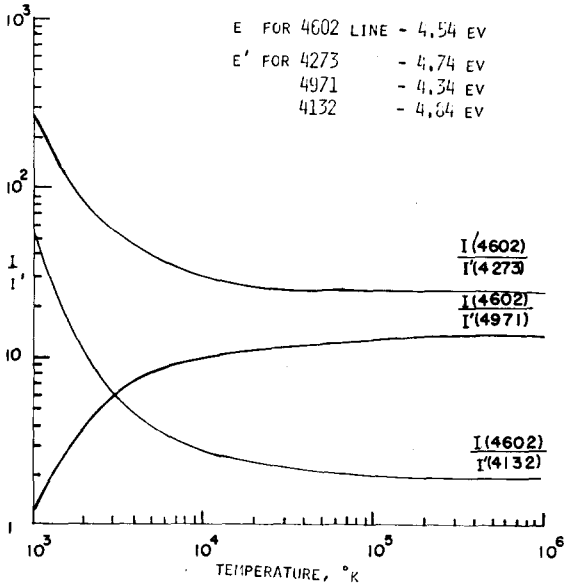

FIG. 14. Calculated intensity ratios of various neutral Li lines as functions of temperature.

D. Streak and Framing Photography of the Plasma

Streak and framing pictures of the plasma (Fig. 17) were used to determine the plasma diameter as a function of time. It was then possible to estimate the total neutral atom density by assuming a uniform particle density in the plasma column.

The framing pictures indicate that the plasma retains a well-defined cylindrical geometry up to about 6 μsec; thereafter, the plasma rapidly disperses.

The streak pictures were taken using a 1-mm-wide slit. The effective length of the wire thus photographed was 1.5 mm at the center of the 1-in.-long wire. In these pictures, oscillations of the wire diameter were observed. The frequency of these oscillations were about 1 MHz which is similar to the oscillations observed in the time-resolved spectra of the emitted radiation from the plasma. (The plasma radiation oscillates at two frequencies, Fig. 8; one at the discharge circuit frequencies, 77 kHz, and the other at a frequency of about 1 MHz.) Since the streak picture of the

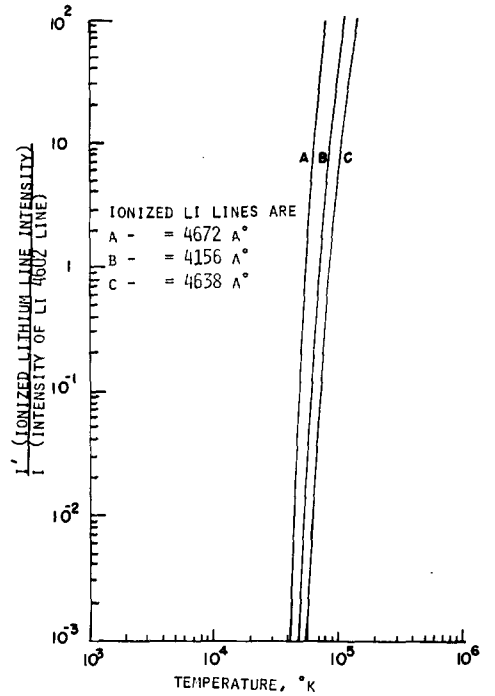

FIG. 15. Calculated ratios of various ionized-Li line intensities to the intensity of Li 4602 line as functions of temperature.

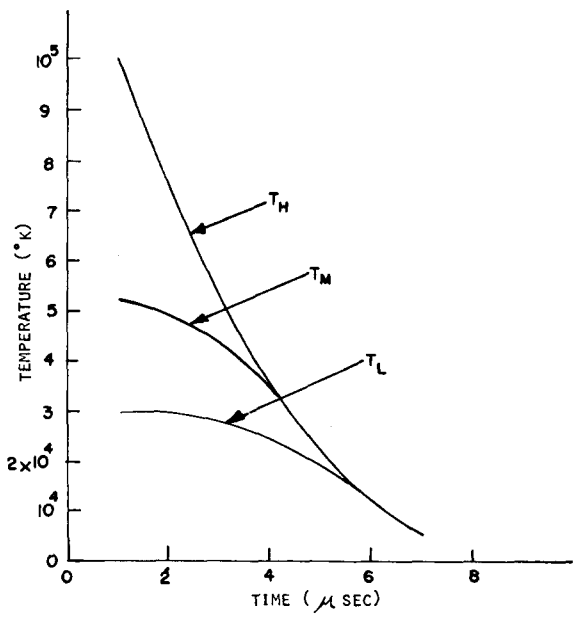

FIG. 16. Assumed temperature variations in the exploding Li-wire plasma (0.0075-cm-diam, 2.5-cm long, $V_0=10$ kV) as functions of time.

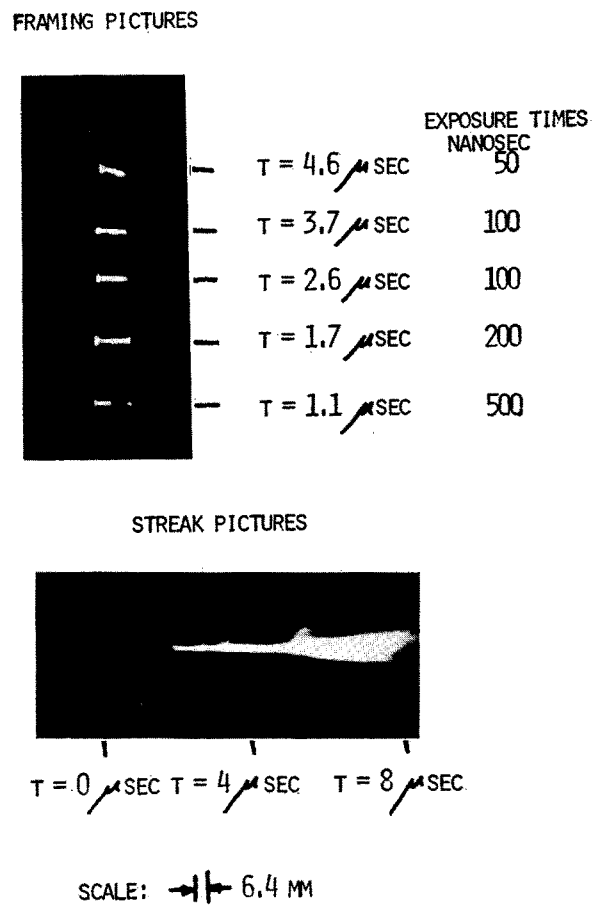

FIG. 17. Framing and streak pictures of the explosion of a 0.0085-cm-diam, 2.5-cm-long Li wire in vacuum with $V_0 = 10$ kV.

plasma and the time-resolved spectra could not be obtained simultaneously with one camera, the coincidence of these oscillations could not be checked. These oscillations may have been due to Z-pinching of the plasma by its self-magnetic field (current in the discharge is as high as 6×10^4 A) and subsequent expansion as a result of high kinetic pressures.

At certain stages of the discharge, the radiation from the entire surface of the plasma column did not appear to be uniform as the edges of the column were brighter than the center. However, these pictures indicate a uniform density cylinder most of the time as has been suggested[36] and not a ring-shaped expansionas has been proposed by Nash and DiSieno.[37]

In Fig. 18 the diameter of the plasma column $L(t)$ is plotted as a function of time based on the measurements of the framing and streak pictures. An average curve is drawn through these points, and labeled $\bar{L}(t)$. The scatter in data about this average is about 20%. The principle of particle conservation was used to obtain the total neutral atom density. Assuming uniform particle density in the plasma column, total particle densities were estimated as a function of time from the measurement of the plasma column diameter. Since the lithium was mainly singly ionized, the ion density was determined from the electron density measurements. The difference between the total particle density and ion density represents the total neutral atom density. In Fig. 13, total neutral density is plotted as a function of time.

E. Measurement of the Absorption of He–Ne Laser Radiation by the Plasma

Two independent measurements indicated that the laser radiation was absorbed in the plasma: that made by the image converter camera of the time-resolved spectra including the wavelength of the laser radiation at 6328 Å, and that made by the photomultiplier attached to the prism monochromator which admitted only the radiation at 6328±20 A. Typical simultaneous recordings of $I_L(t)$ (the intensity of the transmitted laser radiation) by the image converter camera and by the photomultiplier are shown in Fig. 8. In the final analysis of the data the oscilloscope recording of the photomultiplier was used to obtain the value of $I_L(t)$. In Fig. 19, the percentage absorption of the laser radiation, $A(t)$, is shown as a function of time.

As shown in Fig. 8, the intensity of the laser beam was indeed attenuated considerably in passing through the plasma. It had to be ascertained, however, that this attenuation was due to absorption and not due to some other phenomenon such as scattering, reflection, or refraction.

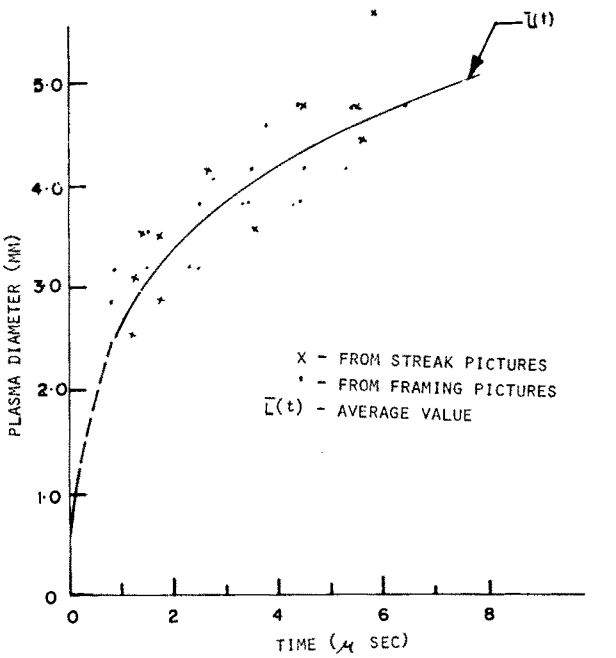

FIG. 18. Measured values of plasma diameter as a function of time.

Since the frequency of the laser radiation, $\nu = 4.75 \times 10^{14}$ sec^{-1}, is considerably higher than the plasma frequencies attained in this experiment ($\nu_p = 1.8 \times 10^{13}$ sec^{-1} when $N_e = 4 \times 10^{18}$ cm^{-3}) reflection and scattering were expected to be negligible.

To investigate the possibility of refraction,[38] the laser radiation transmitted by the plasma was directly photographed by the image converter camera. All optical components between the plasma and the camera including the objective lens of the camera were removed. About 0.8-mrad beam deviation was observed only in the plane perpendicular to the axis of the wire and was expected since the deviation depends on the gradient of the electron density. Beam deviation was not observed in the plane of the wire axis. The deviation in the vertical plane could not affect the detection of the laser beam by the system including the spectrograph and the image converter camera.

Absorption measurements were also made with the laser beam passing a few millimeter below the wire. Typical recordings of the laser intensity $I_L(t)$ are shown in Fig. 20. The further away from the wire axis the laser beam was moved, the longer it took for the plasma to reach the beam, and the later the absorption began. These pictures clearly indicate that the attenuation of the laser radiation intensity in the plasma was due to the interaction of laser radiation with the plasma.

In summary, a plasma was produced by exploding a 0.0075-cm-diam, 2.5-cm-long Li wire in vacuum, by discharging a 13.8-μF capacitor charged to 10 kV. A He–Ne laser beam of 6328 Å was passed through it. The absorption of its radiation in the plasma was measured. In order to calculate the expected absorption in this plasma, the following parameters were measured or estimated: electron density, $N_e(t)$; electron temperature, $T(t)$; plasma diameter, $L(t)$; and total neutral atom density $N_n(t)$.

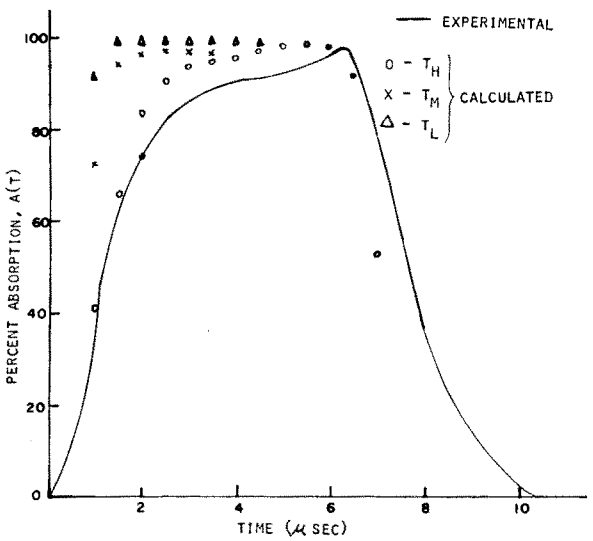

FIG. 19. Measured and calculated values of percent absorption as functions of time.

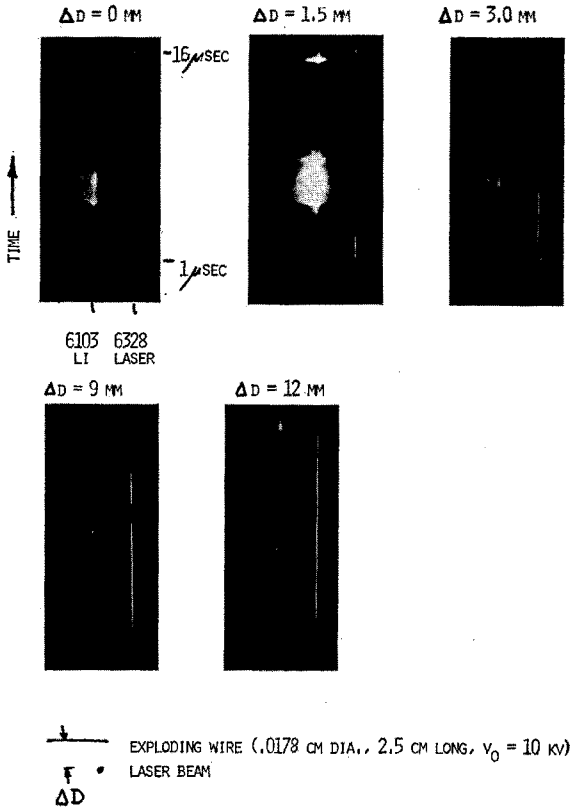

FIG. 20. Off-axis measurement of the absorption of He–Ne laser radiation for various values of ΔD.

IV. RESULTS AND CONCLUSIONS

In Table I, the experimental results and the calculated values are tabulated. This table has three main sections. In the first section, the measured values of $N_e(t)$, $N_n(t)$, and $\bar{L}(t)$ are given for values of t from 1 to 7 μsec. These values were obtained from the curves given in Figs. 13 and 18. The data begin at $t = 1$ μsec because the recordings of the spectra and streak pictures of the plasma, which were obtained with the image converter camera, started 1 μsec after the discharge was initiated.

The second section of Table I presents the measured values of percentage absorption, $A(t)$, and the average experimental values of the total absorption coefficients, $\bar{\alpha}_T{}^E$. These values of $\bar{\alpha}_T{}^E$ were obtained by dividing the values of $\ln\{1-[A(t)/100]\}$ by the average values of the plasma diameter, $\bar{L}(t)$.

In the third section of Table I, the calculated values of percentage absorption and absorption coefficients are given for three different temperatures (T_H, T_M, T_L) at each stage of the explosion. Since the temperature could not be measured accurately (10 000°–50 000°K; see Sec. III.C) as a function of time, it was necessary

TABLE I. Summary of data on absorption measurements.

Time	Experimentally measured values of plasma parameters			Experimentally measured values of absorption		Calculated values of absorption					
t (μsec)	$N_e(t)$ (cm^{-3})	$\bar{N}_n(t)$ (cm^{-3})	$\bar{L}(t)$ (cm)	$A(t)$ (%)	$\bar{\alpha}_T{}^E$ (cm^{-1})	$T(t)$ (°K)	$K_{\nu}{}^{ff}$ (cm^{-1})	α_N (cm^{-1})	α^{PI} (cm^{-1})	$\alpha_T{}^c$ (cm^{-1})	$A^c(t)$ (%)
1.0	5×10^{17}	3.8×10^{19}	0.265	38	1.81	10^5	0.00095	0.0684	1.86	1.94	40.2
						5.2×10^4	0.002	0.156	4.74	4.90	72.6
						3×10^4	0.0037	0.228	9.20	9.43	92
1.5	2.1×10^{18}	2.5×10^{19}	0.310	63	3.21	8.8×10^4	0.0198	0.228	3.25	3.50	66.2
						5.1×10^4	0.038	0.420	8.24	8.68	94.2
						3×10^4	0.066	0.683	15.91	16.66	99.4
2.0	3.4×10^{18}	1.9×10^{19}	0.340	74	3.96	7.7×10^4	0.0165	0.315	5.09	5.47	84.4
						5.0×10^4	0.102	0.503	9.04	9.65	96.2
						3×10^4	0.174	0.806	16.2	17.18	99.7
2.5	4.1×10^{18}	1.55×10^{19}	0.365	81	4.54	6.5×10^4	0.109	0.368	6.08	6.56	90.8
						4.7×10^4	0.141	0.546	9.51	10.20	97.6
						2.9×10^4	0.261	0.814	15.33	16.41	99.7
3.0	4.1×10^{18}	1.3×10^{19}	0.385	86	5.11	5.4×10^4	0.134	0.372	6.82	7.33	94
						4.4×10^4	0.168	0.468	8.60	9.24	97.1
						2.8×10^4	0.260	0.720	13.06	14.04	99.6
3.5	3.6×10^{18}	1.2×10^{19}	0.405	89	5.46	4.4×10^4	0.129	0.379	6.89	7.40	95
						4×10^4	0.156	0.418	7.77	8.34	96.6
						2.7×10^4	0.214	0.582	11.06	11.85	99.2
4.0	3.1×10^{18}	1.13×10^{19}	0.420	90	5.48	3.6×10^4	0.120	0.385	7.36	7.87	96.2
						3.5×10^4	0.120	0.385	7.36	7.87	96.2
						2.5×10^4	0.168	0.508	10.5	11.2	99.1
4.5	2.6×10^{18}	1.09×10^{19}	0.435	91	5.54	2.8×10^4	0.108	0.396	8.11	8.61	97.6
						2.8×10^4	0.108	0.396	8.11	8.61	97.6
						2.3×10^4	0.128	0.452	9.73	10.31	98.8
5.0	2.1×10^{18}	1.06×10^{19}	0.450	93	5.92	2.2×10^4	0.086	0.378	8.94	9.40	98.5
						2.2×10^4	0.086	0.378	8.94	9.40	98.5
						2.1×10^4	0.086	0.378	8.94	9.40	98.5
5.5	1.65×10^{18}	1.03×10^{19}	0.460	94	6.12	1.7×10^4	0.065	0.34	9.00	9.41	98.7
						1.7×10^4	0.065	0.34	9.00	9.41	98.7
						1.7×10^4	0.065	0.34	9.00	9.41	98.7
6.0	1.25×10^{18}	1.01×10^{19}	0.472	96	6.83	1.3×10^4	0.047	0.289	8.04	8.38	98.1
						1.3×10^4	0.047	0.289	8.04	8.38	98.1
						1.3×10^4	0.047	0.289	8.04	8.38	98.1
6.5	8.8×10^{17}	1×10^{19}	0.484	97	7.23	9.5×10^3	0.030	0.176	4.98	5.19	91.9
						9.5×10^3	0.030	0.176	4.98	5.19	91.9
						9.5×10^3	0.030	0.176	4.98	5.19	91.9
7.0	6×10^{17}	9.9×10^{18}	0.495	78	3.46	7×10^3	0.017	0.083	1.43	1.53	53
						7×10^3	0.017	0.083	1.43	1.53	53
						7×10^3	0.017	0.083	1.43	1.53	53

$\bar{N}_n(t)$ average value of total neutral atom density
$\bar{L}(t)$ average value of plasma column diameter
$A(t)$ measured value of absorption (in percent)
$\bar{\alpha}_T{}^E(t)$ average value of total absorption coefficient $\alpha_T{}^E(t)$
$T(t)$ assumed values of temperatures: T_H, T_M, and T_L (see Fig. 16)
α^{PI} net absorption coefficient of photoionization (Figs. 5 and 6)
$\alpha_T{}^c$ calculated value of total absorption coefficient $\alpha_T{}^c = K_{\nu}{}^{ff} + \alpha_n + \alpha^{PI}$
$K_{\nu}{}^{ff}$ Net absorption coefficient of inverse bremsstrahlung in the presence of ions (Fig. 1)
α_N net absorption coefficient of inverse bremsstrahlung in the presence of neutral atoms (Fig. 1)
$A^c(t)$ Calculated value of percent of absorption $A^c(t) = \{1-\exp\lfloor-\alpha_T{}^c(t)\bar{L}(t)\rfloor\}$

to show how the calculated absorption coefficients varied with temperature. The calculated values of the absorption coefficients for inverse bremsstrahlung in the presence of ions and neutrals (K_ν^{II} and α_N) and those of photoionization (α^{PI}) were obtained from the curves in Figs. 1, 5 and 6. The calculated values of the total absorption coefficient, $\alpha_T{}^C$, were obtained by summing the absorption coefficient for the three mechanisms; that is, $\alpha_T{}^C = K_\nu^{II} + \alpha_n + \alpha^{PI}$. The calculated values of percentage were obtained using the following equation

$$A^c(t) = [1 - \exp(-\alpha_T{}^c \bar{L}(t)] \times 100. \qquad (17)$$

The values of $A^c(t)$ are shown in Fig. 19 in order to compare them with the experimental values. The measured and calculated values of total absorption coefficients differed at most by a factor of five. Even though this discrepancy may seem large, it represents a significant improvement over the results reported by Litvak and Edwards[7] and by Lampis and Brown.[8]

In order to check the error in the calculated values of percent absorption $A^c(t)$ due to the scatter in the values of $L(t)$ and $N_n(t)$, a number of calculations of $A^c(t)$ were made using the data from individual points. There was at most a 20% scatter in the results.

The factor-of-five discrepancy may be due to the approximations in the calculations. The main uncertainty in these calculations is in the value of n^* (hence the partition function), and it affects the photoionization absorption coefficient significantly. Another uncertainty may be in the use of hydrogenic calculations for Li. It should be pointed out again that we have assumed a plasma of uniform density.

The reproducibility of the absorption measurements was good. In Fig. 21, absorption curves obtained from a number of explosions with the same experimental conditions are plotted. In Fig. 22 repeatability in the time resolved spectra, including Li 6103 and the He–Ne laser radiation at 6328 Å, is shown. The variation in the absorption data and in the spectra during the first few microseconds was small, while the variations after about 6 μsec were more pronounced. This was because the instability and breakup of the plasma after about 6 μsec was not repeatable, and the spectra and absorption in the plasma were significantly affected by the variations in the shape of the plasma column.

The results of these calculations and experiments also showed that the contribution of neutral atoms to the photon absorption through inverse bremsstrahlung was much larger than that of the ions. Due to the large absorption by photoionization, however, the contribution of neutral atoms could not be isolated in this experiment. The results of preliminary calculations indicate that the contribution of neutral atoms to the absorption through inverse bremsstrahlung could be measured with a percentage ionization of less than 10%

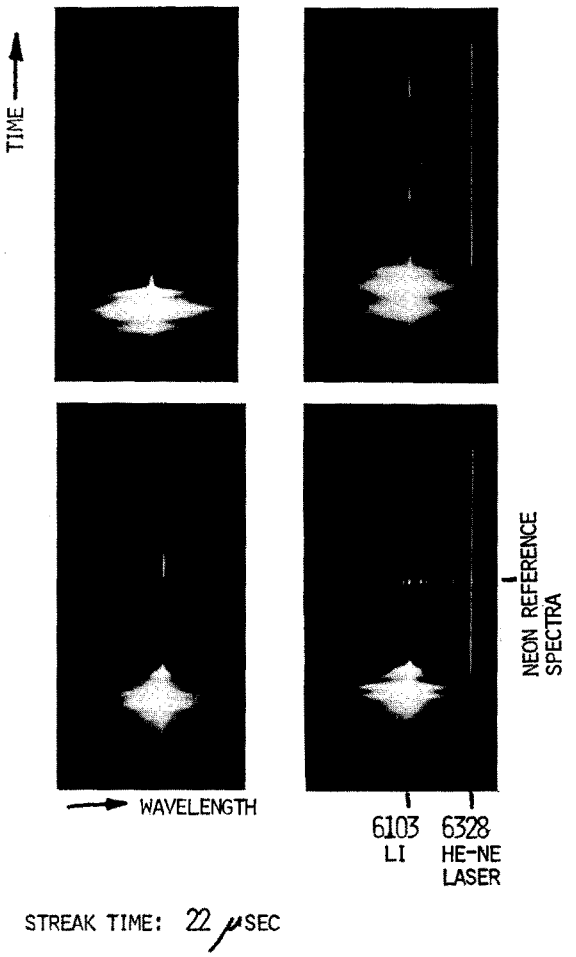

FIG. 22. Repeatability of the time-resolved spectra.

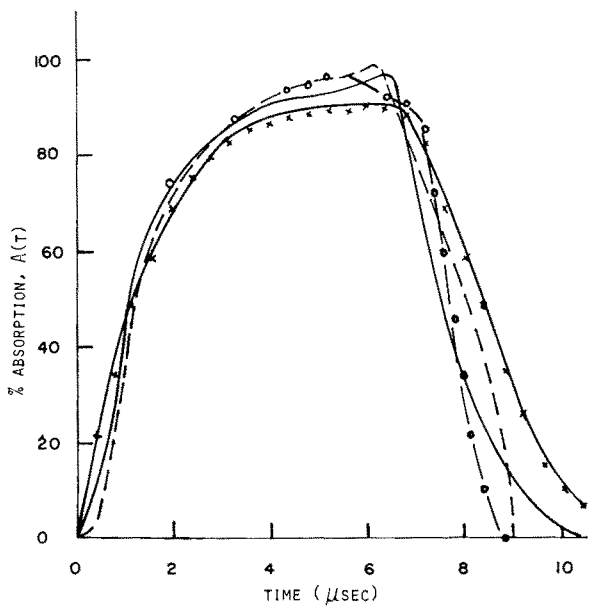

FIG. 21. Repeatability of the absorption measurements.

and at temperatures below 5000°K. These conditions could be attained in exploding wire plasmas.

ACKNOWLEDGMENTS

The authors would like to thank Professor A. Ziya Akcasu and Professor Robert K. Osborn and Dr. Hsian-Shi Tsai for the valuable discussions. They are also grateful to Mr. Tom A. Leonard and Mr. Gregg Smith for their suggestions and assistance in the experimental work.

* This work was supported in part by the Advanced Research Projects Agency (Project DEFENDER) and was monitored by the U.S. Army Research Office–Durham, and by the Air Force Office of Scientific Research, Office of Aerospace Research.

† Based in part upon a thesis submitted by Erol Oktay to The University of Michigan in partial fulfillment of the requirements for the degree of Doctor of Philosophy. Partial support was obtained from the GE Foundation.

‡ Present address: Department of Nuclear Engineering, M.I.T., Cambridge, Mass. 02139.

[1] R. G. Meyerand, Jr., and A. F. Haught, Phys. Rev. Lett. **11,** 401 (1963).
[2] P. E. Faugeras, M. Mattioli, and R. Papoular, Plasma Phys. **10,** 939 (1968).
[3] R. E. Kidder, Nucl. Fusion **8,** 3 (1968).
[4] R. G. Meyerand and A. F. Haught, Phys. Rev. Lett. **13,** 7 (1964).
[5] R. W. Minck and W. G. Rado, *Physics of Quantum Electronics* (McGraw-Hill Book Co., Inc., New York, 1966).
[6] J. K. Wright, Proc. Phys. Soc. (London) **84** (1964).
[7] M. M. Litvak and D. F. Edwards, J. Appl. Phys. **37,** 4462 (1966).
[8] G. Lampis and Sanborn C. Brown, Phys. Fluids **11,** 1137 (1968).
[9] H. S. Tsai, Z. Akcasu, and R. K. Osborn, "Contribution of Neutral Atoms to the Absorption of Photons in Plasma," Tech. Rep., 07599-18-T, Coll. of Eng. The Univ of Mich., Aug. 1968.
[10] H. S. Tsai, E. Oktay, and Z. Akacsu (unpublished).
[11] A. W. Weiss, Phys. Rev. **166,** 70 (1968).
[12] B. Ya'akobi, Phys. Lett. **23,** 655 (1966).
[13] R. Woolley and D. W. N. Stibbs, *The Outer Layers of a Star,* 62 (Clarendon Press, Oxford, England, 1953).
[14] Ya B. Zel'dovich and Yu B. Raizer, *Physics of Shock Waves and High Temperature Hydrodynamics Phenomena* (Academic Press Inc., New York, 1966), Vol. 1.
[15] W. S. Karzas and R. Latter, Astrophys. J. Suppl. Ser. **6,** 167 (1961-62).
[16] S. Chandrasekhar and F. H. Breen, Astrophys. **J. 103,** 41 (1946).
[17] J. A. Wheeler and R. Wildt, Astrophys. J. **95,** 282 (1942).
[18] T. Ohmura and H. Ohmura, Phys. Rev. **121,** 8 (1961).
[19] Z. Akcasu and L. H. Wald, Phys. Fluids **10,** 1327 (1966).
[20] O. B. Firsov and M. I. Chibisov, Sov. Phys.—JETP **12,** 1235 (1961).
[21] B. Kivel, J. Quant. Spectrosc. Radiative Transfer **17,** 27 (1967).
[22] R. C. Mjolsness and H. M. Ruppel, J. Quart. Spectrosc. Radiative Transfer **7,** 423 (1967).
[23] J. Cooper, Rep. Progr. Phys. **24,** 45 (1966).
[24] H. R. Griem, *Plasma Spectroscopy* (McGraw-Hill Book Co., Inc., New York, 1964).
[25] J. L. Jackson and L. S. Klein, Phys. Rev. **177,** 352 (1969).
[26] M. McChesney, Can. J. Phys. **42,** 2473 (1964).
[27] A. V. Potapov and G. V. Babkin, High Temp. **5,** 217 (1967).
[28] H. W. Drawin and P. Felenbok, *Data for Plasma in Local Thermodynamic Equilibrium* (Gauthier-Villars, Paris, 1965).
[29] W. L. Wiese, M. W. Smith, and B. M. Glennon, *Atomic Transition Probabilities,* Vol. 1, NSRDS-NBS-4 (May 20, 1966).
[30] K. Gezalov and A. V. Ivanova, High Temp. **6,** 400 (1968).
[31] B. Ya'akobi, Proc. Phys. Soc. (London **92,** 100 (1967).
[32] E. Oktay, D. R. Bach, and W. V. Rekewitz, Rev. Sci. Instrum. **39,** 924 (1968).
[33] T. A. Leonard and D. R. Bach, Rev. Sci. Instrum. **39,** 1374 (1968).
[34] T. A. Leonard, Rev. Sci. Instrum. (to be published).
[35] R. D. Cowan and G. H. Dieke, Rev. Mod. Phys. **20,** 418 (1948).
[36] B. Ya'akobi, A. S. Kaufman, and P. Avivi, Proc. Seventh Int. Conf. Phenomena Ionized Gases, I, Belgrade, 1965.
[37] R. P. DeSieno and C. P. Nash, in *Exploding Wire* (Plenum Press, Inc., New York, 1968), Vol 4.
[38] I. S. Falconer and S. A. Ramsden, J. Appl. Phys. **39,** 3449 (1968).